

- and R. B. Saillant, *Chem. Rev.*, **72**, 231 (1971); (b) W. E. Trout, *J. Chem. Educ.*, **15**, 77 (1938).
- (14) (a) W. Heiber and F. Leutert, *Naturwissenschaften*, **19**, 360 (1931); (b) W. Reppe and H. Vetter, *Justus Liebigs Ann. Chem.*, **582**, 133 (1953).
- (15) A. C. Harkness and J. Halpern, *J. Am. Chem. Soc.*, **83**, 1258 (1961).
- (16) E. L. Muetterties, *Inorg. Chem.*, **4**, 1841 (1965).
- (17) D. J. Darensbourg and J. A. Froelich, *J. Am. Chem. Soc.*, **99**, 5941 (1977).
- (18) A. J. Deeming and B. L. Shaw, *J. Chem. Soc. A*, 443 (1969).
- (19) H. C. Clark, K. R. Dixon, and W. J. Jacobs, *J. Am. Chem. Soc.*, **91**, 1346 (1969).
- (20) F. A. Cotton and G. Wilkinson, "Advanced Inorganic Chemistry", 3rd ed., Wiley, New York, 1972.
- (21) J. L. Dawes and J. D. Homes, *Inorg. Nucl. Chem. Lett.*, **7**, 847 (1971).
- (22) B. F. G. Johnson, J. Lewis, and I. G. Williams, *J. Chem. Soc. A*, 901 (1970).
- (23) S. A. R. Knox, J. W. Koepke, M. A. Andrews, and H. D. Kaesz, *J. Am. Chem. Soc.*, **97**, 3942 (1975).
- (24) D. B. Yawney and F. G. A. Stone, *J. Chem. Soc. A*, 502 (1969).
- (25) B. R. James, G. L. Rempel, and W. K. Teo, *Inorg. Synth.*, **16**, 49 (1976).
- (26) D. K. Huggins, W. Fellmann, J. M. Smith, and H. D. Kaesz, *J. Am. Chem. Soc.*, **86**, 4841 (1964).
- (27) (a) M. Iwata, *Nagoaka Kogyo Tanki*, **4**, 307 (1968); *Chem. Abstr.*, **70**, 76989 (1969); (b) "Encyclopedia of Chemical Technology", Vol. 10, 2nd ed., Wiley, New York, 1972, p 101.
- (28) J. Knight and M. J. Mays, *J. Chem. Soc., Dalton Trans.*, 1023 (1972).
- (29) (a) J. R. Wilkinson and L. J. Todd, *J. Organomet. Chem.*, **118**, 199 (1976); (b) H. A. Hodeli, D. F. Shriver, and C. A. Ammlung, *J. Am. Chem. Soc.*, **100**, 5239 (1978).
- (30) H. Cohen and P. C. Ford, work in progress.
- (31) A likely candidate for this species is the anionic carbide complex $\text{Ru}_6\text{C}(\text{CO})_{16}^{2-}$ since its IR spectrum is consistent with that of the reaction product of KOH plus $\text{Ru}_6\text{C}(\text{CO})_{17}$ in aqueous ethoxyethanol (2034 w, 2016 w, 1976 vs, 1950 sh, s, 1920 w, 1790 w cm^{-1}). The latter spectrum is reminiscent of the IR spectrum of the iron species $\text{Fe}_6\text{C}(\text{CO})_{16}^{2-}$ (1964 s, 1957 sh, 1930 sh, 1775 w cm^{-1}).³³
- (32) M. R. Churchill, J. Wormold, J. Knight, and M. J. Mays, *J. Am. Chem. Soc.*, **93**, 3073 (1971).
- (33) J. R. Graham and R. J. Angelici, *Inorg. Chem.*, **6**, 2082 (1967).
- (34) A. Poe and M. V. Twigg, *Inorg. Chem.*, **13**, 2982 (1974).
- (35) D. R. McAlister, D. K. Erwin, and J. E. Bercaw, *J. Am. Chem. Soc.*, **100**, 5967 (1978).
- (36) D. Gross and P. C. Ford, unpublished results.
- (37) J. R. Shapley, J. B. Keister, M. R. Churchill, and B. G. DeBoer, *J. Am. Chem. Soc.*, **97**, 4145 (1975).
- (38) J. R. Moss and W. A. G. Graham, *J. Chem. Soc., Dalton Trans.*, 89 (1977).
- (39) J. D. Cotton, M. I. Bruce, and F. G. A. Stone, *J. Chem. Soc. A*, 2162 (1968).
- (40) For example, if trinuclear Ru_3 cluster were solely responsible for the catalysis yet the vast majority of ruthenium were present in Ru_4 clusters and a labile $4\text{Ru}_3 \rightleftharpoons 3\text{Ru}_4$ equilibrium were extant under catalysis conditions, then the kinetic order in $[\text{Ru}_{\text{total}}]$ would be 0.75. The reverse case would give an order of 1.33. The presence of significant equilibrium concentrations of both types of clusters (as seen in the present case) would give an apparent order between these two limits as would be the case when both types of clusters have comparable activities for the shift reaction. Given that the range of activities noted for WGS catalysis by various group 8 metal carbonyls is relatively narrow, it certainly does not seem unreasonable that clusters of the same metal but of different nuclearities would have comparable reactivities.
- (41) G. Geoffroy, private communication, submitted for publication.

Autoxidation of Transition-Metal Complexes. Reaction of a 1:1 Cobalt–Molecular Oxygen Complex with Acids to Yield Hydrogen Peroxide. Kinetics and Mechanism

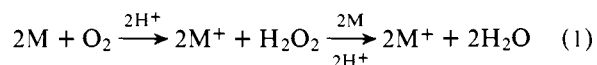
Joseph J. Pignatello[†] and Frederick R. Jensen*

Contribution from the Department of Chemistry, University of California, Berkeley, California 94720. Received December 12, 1978

Abstract: Dioxxygen (pyridine)-*N,N'*-ethylenebis(acetylacetoniminato)cobalt(II) reacts with acids in organic solvents containing excess pyridine to give 0.5 mol of molecular oxygen, 0.5 mol of hydrogen peroxide, and 1 mol of dipyridine *N,N'*-ethylenebis(acetylacetoniminato)cobalt(III) ion as an ion pair with the anion of the acid. In pyridine below 0 °C the reaction proceeds quantitatively within experimental uncertainty, and no detectable buildup of intermediates is observed. Kinetic studies were done with acetic acid in pyridine at -10.7 °C by monitoring the evolution of oxygen at constant pressure. The empirical rate law is found to be second order in the cobalt oxygen complex, inverse first order in oxygen pressure, inverse one-half order in cobalt(III) acetate product, and between second and third order in acetic acid. This law holds throughout the course of the reaction, strongly indicating that only one mechanism is in operation. The effect of added bromide and acetate salts on the rate and the demonstrated occurrence of the homoconjugation equilibrium for acetate, $\text{OAc}^- + \text{HOAc} \rightleftharpoons \text{H}(\text{OAc})_2^-$, lead to the conclusion that the high empirical order in acetic acid is equivalent to a first-order dependence each on acetic acid and free, dissociated pyridinium ion. The proposed mechanism involves protonation, and subsequent dissociation as hydrogen peroxide, of the bridging dioxxygen ligand from a binuclear complex intermediate, $\text{pyCo}(\text{acacen})\text{O}_2\text{Co}(\text{acacen})\text{py}$, which exists in rapid equilibrium with the starting mononuclear dioxxygen complex. The involvement of both acid species in the transition state is discussed. The absence of free-radical intermediates was strongly indicated by the results of experiments carried out in the presence of organic radical scavengers and by ESR spectroscopy. The reaction is discussed in terms of autoxidation of transition-metal complexes.

Introduction

Autoxidation reactions of transition-metal complexes are represented by the equation

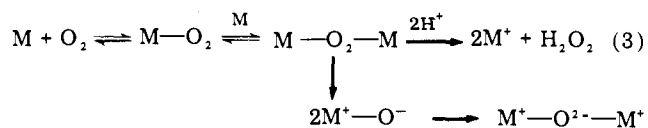
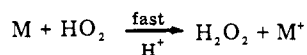
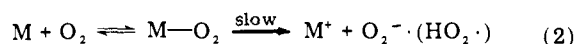


where M represents the ligated metal in the reduced state. The initial product, hydrogen peroxide, is usually not observed

[†] Gray Freshwater Biological Institute, University of Minnesota, Navarre, Minn. 55392.

because it rapidly oxidizes two more metal ions. Most of the investigative work into mechanism has been done on first-row transition metals: Ti(III), V(II, III, IV), Cr(II), Mn(II), and most frequently Fe(II), Co(II), and Cu(I). The mechanisms that have been invoked for the production of hydrogen peroxide in the first step fall into two categories. In eq 2 dissociation of an initial oxygen adduct of the metal complex into oxidized metal and superoxide ion or the hydroperoxyl radical ($\text{p}K_a$ of HO_2^\cdot is 4.88¹) occurs which is then followed by fast oxidation of another metal complex by $\text{O}_2^{\cdot-}$ (HO_2^\cdot).²⁻⁵ Evidence other than kinetics for this scheme is lacking; in particular the species

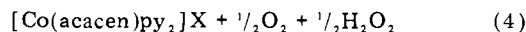
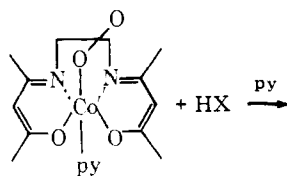
$O_2^- \cdot$ ($HO_2^- \cdot$) has not been directly observed in these cases. It has been suggested that the kinetics—first order in metal and O_2 —are also in agreement with the mechanism in eq 3 with the first step as rate limiting.^{6,7}



Equation 3 features an intermediate binuclear molecular oxygen adduct. Protonation and then dissociation can occur giving hydrogen peroxide and oxidized metal complex.⁶⁻¹¹ Alternatively, the binuclear oxygen adduct can dissociate homolytically to yield an oxo metal species which is either stable^{12,13} or rapidly oxidizes another metal to form the μ -oxo complex.^{7,14-18} Evidence for these mechanisms includes kinetics—second order in metal and first order in O_2 —and the known propensity of complexes of some of these metals to form the binuclear molecular oxygen adducts.

It is significant that the initial step in all of these mechanisms is coordination of oxygen. A large number of oxygen adducts have been prepared from complexes of Cu(I), Co(II), Fe(II), Mn(II), Cr(II), Ni(0), and several of the second- and third-row transition metals. A number of reviews¹⁹ and papers²⁰ have described these. The electronic structure of the metal-dioxygen bond in all cases involves a transfer of some electron density from the metal to the dioxygen, giving rise to three formal designations: bent, end-on superoxide ($M^+O_2^- \cdot$), edge-on peroxide ($M^2+O_2^{2-}$), and μ -peroxo ($M^+-\bar{O}-\bar{O}-M^+$). Coordination of oxygen or reduced dioxygen is also a central feature of many metalloprotein and metalloenzyme reactions including those of oxygen transport proteins, cytochromes, oxidases, and oxygenases, and the related peroxidases, catalases, and superoxide dismutases. The structures of the metal- O_2 units in these biological systems appear to fit into the three categories above. The fate of bound oxygen is an important matter as it relates to the reaction mechanisms of these systems. Autoxidation can be considered as the elementary reaction of transition-metal complexes with molecular oxygen and may provide valuable insight.

The cobalt complex used in this study is *N,N'*-ethylenebis(acetylacetoniminato)cobalt(II), which forms quantitatively and reversibly a well-known^{19d,21,22} 1:1 oxygen complex of the "superoxide" type (shown below) in the presence of a Lewis base which can coordinate in the sixth position. The decomposition of a 1:1 oxygen complex of this type to oxidized metal and reduced oxygen products has not been studied previously. Reaction of this oxygenated complex with general acids HX in pyridine and other organic solvents was observed to produce oxygen and hydrogen peroxide, according to eq 4. In this me-



(The designation acacen for the equatorial ligand will henceforth be omitted.)

dium hydrogen peroxide is relatively stable.

In all autoxidation reactions studied so far, the 1:1 complex has been present only as a transient intermediate, thus precluding much information to be gained on the steps following oxygenation. Beginning with a fully oxygenated metal complex, this system allows a probe of the steps that follow.

Results and Discussion

A. Stoichiometry. Solutions of Co(II) in pyridine or in toluene containing several equivalents of pyridine below 0 °C and under 1 atm of oxygen have been found to absorb 1.00 mol ($\pm 2\%$) of oxygen in accord with the results of previous work.^{22,23} At warmer temperatures the oxygen adduct slowly decomposes to give products which are apparently difficult to define.²² The equilibrium constant for oxygenation has been found to be $6.6 \times 10^4 M^{-1}$ in pyridine at 20 °C by Amiconi et al.²³ Using their thermodynamic parameters it can be calculated that the ratio of oxygenated to unoxoxygenated cobalt is $5.8 \pm 1.5 \times 10^3$ in pyridine at -10.7 °C and under 1 atm of oxygen, which are the conditions under which the kinetics and most of the other experiments in this work were carried out.

Addition of acids, HX, to solutions of preformed $pyCoO_2$ in pyridine or toluene results in the reaction given in eq 4. The experimentally determined quantity of oxygen liberated on introduction of 1–20 mol of acetic, *p*-toluenesulfonic, hydrochloric, or hydrobromic acid was found to be 0.49 ± 0.02 mol. The cobalt product isolated from the reaction mixture after addition of 1 equiv of aqueous HBr is the salt $[Co^{II}py_2]Br$ which was identified by a satisfactory elemental analysis and by comparison of its absorption spectrum with that of authentic material.²⁴ The absorption spectrum of the reaction mixture immediately after completion is identical with that of the compound isolated.

The proton magnetic resonance (1H NMR) spectrum of $[Co^{II}py_2]Br$ is substantially the same in $CDCl_3$, pyridine- d_5 , or D_2O : a singlet for the methine hydrogens (δ 5.0), a singlet for the bridging methylene hydrogens (δ 3.9), and a singlet for each of the two different methyl groups (δ 2.2, 2.3). The aromatic region in $CDCl_3$ shows the resonances corresponding to two pyridine molecules per cobalt in a pattern which is uncharacteristic of free pyridine. This ratio persists despite extensive drying of the solid, indicating that the structural characterization of the compound is correct; namely, that two pyridines are bound axially to the cobalt and the bromide is the counterion in the outer coordination sphere. The isolated product of the reaction with acetic acid (HOAc) displays the same absorption spectrum in pyridine and the identical 1H NMR spectrum in both pyridine- d_5 and D_2O as $[Co^{II}py_2]Br$ except for the presence of methyl protons of acetate, indicating its structure to be the complex salt as well.

Hydrogen peroxide or a species which behaves similarly was determined in the reaction with acetic acid in pyridine by the following experiments. (1) A spot test specific for H_2O_2 utilizing the color change when phenolphthalin is oxidized to phenolphthalein in aqueous sodium hydroxide in the presence of $CuSO_4$ ²⁵ was strongly positive. (All proper blanks and sensitivity tests were run.) (2) When aqueous $KMnO_4$ was injected after completion of the reaction, 0.48–0.49 mol of O_2 was evolved corresponding to 96–98% yield based on eq 4 and the known quantitative oxidation of H_2O_2 by permanganate.^{26a} (3) When a slurry of 5% platinum on carbon in pyridine was added, 0.23 mol or 92% of the amount of oxygen expected by the reaction in eq 4 was evolved based on the known catalytic decomposition of H_2O_2 to oxygen and water.^{26b} (4) Extraction of the reaction mixture, to which 10 volumes of $CHCl_3$ had been added after the reaction had gone to completion, with 40% aqueous sodium acetate (w/v) and titration iodometrically

Table I. Results of Kinetic Runs to Determine the Empirical Orders in Acetic Acid, pyCoO₂, and Product

| order in | no. of data sets | no. of runs used in data sets ^c | av order ^d | av corr coeff |
|---------------------------------|------------------|--|-----------------------|---------------|
| acetic acid ^a | 9 | 4-7 | 2.39 ± 0.05 | 0.9990 |
| pyCoO ₂ ^b | 18 | 3-6 | 2.09 ± 0.06 | 0.9996 |
| product ^b | 13 | 4-6 | -0.50 ± 0.04 | 0.9959 |

^a [pyCoO₂]₀ = 4.25 × 10⁻³ M, [HOAc]₀ = 2.9–15.6 × 10⁻² M.

^b [HOAc]₀ = 8.93 × 10⁻² M, [pyCoO₂]₀ = 1.77–11.8 × 10⁻³ M.

^c The number of runs used to calculate the order is not the same for each set because of the reliability of the data in certain regions of the reaction curves; i.e., some runs were too fast at low conversion for an accurate rate to be determined while others were too slow at high conversion. ^d The standard deviations shown are the averages of the standard deviations of the data sets. The average order and standard deviation are weighted by the number of runs used.

yielded 72% of the expected hydrogen peroxide. Concentrated sodium acetate is needed to cause phase separation and to salt out [Co^{III}py₂]OAc, which is very soluble in water and which otherwise would interfere with the determination. Control experiments determined that chloroform was needed to prevent hydrogen peroxide from remaining in the pyridine phase.

(5) Finally, simple distillation of the reaction mixture in pyridine at 0 °C under vacuum and titration of the distillate iodometrically yielded 6–8% of the expected hydrogen peroxide. The low values are the result of decomposition of hydrogen peroxide by the cobalt(III) product, which assumes significance as the solution becomes more and more concentrated during the distillation and by the unfavorable difference in the boiling points between H₂O₂ (156 °C) and pyridine (115 °C). The former effect was verified in control experiments using the synthetically prepared cobalt complex salt (see Experimental Section) and hydrogen peroxide. Attempts were made to rectify the latter problem by using solvents of higher boiling point (DMF, 153 °C; 3,5-lutidine, 172 °C; 4-*tert*-butylpyridine, 198 °C; quinoline, 242 °C). Distillation of dilute hydrogen peroxide (2–5 × 10⁻² M, the approximate concentration expected from the reaction) from these solvents is not very efficient; only 9 (from DMF) to 19% (from quinoline) was obtained in the first half of the solution distilled. Little or no reaction occurred between solvent and hydrogen peroxide under the conditions. The use of 4-*tert*-butylpyridine as the solvent in the reaction under study resulted in a yield of 18.6% of the expected hydrogen peroxide in the distillate. Evidence against coordination of peroxide to the product cobalt(III) species, as one explanation for the low yields, is strongly suggested by the fact that addition of hydrogen peroxide to a solution of either [Co^{III}py₂]Br or [Co^{III}py₂]OAc·H₂O²⁷ in pyridine causes no change in the absorption or ¹H NMR spectra.

The ¹H NMR spectrum of the reaction mixture with acetic acid immediately after completion shows the acetate methyl singlet broadened and shifted as far as 3.1 ppm downfield from its normal position at δ 2.3–2.4. This was later found to be due to small amounts of paramagnetic cobalt(II) compound(s) other than unreacted starting material. These could be impurities in the starting material or arise from a side reaction.

B. Kinetics. Determination of the Empirical Rate Law. The reaction of pyCoO₂ with strong acids is very fast but with acetic acid the rate is sufficiently slow to monitor by measuring oxygen evolution. The kinetics were run in pyridine at -10.7 ± 0.1 °C at constant pressure of oxygen gas by injecting a

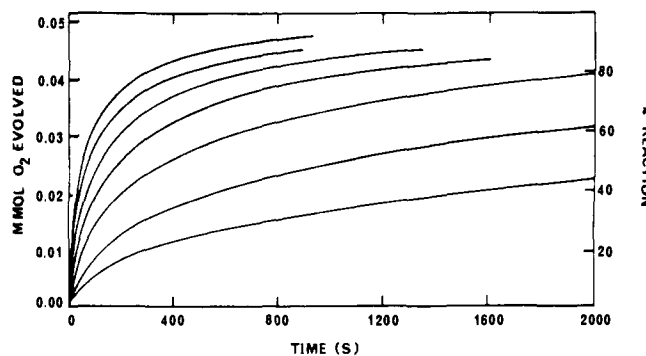


Figure 1. Reaction curves at the same initial [pyCoO₂] (4.25 × 10⁻³ M) and constant pressure of O₂ (1 atm) at -10.7 °C. From top to bottom: initial [HOAc] = 15.6, 13.4, 11.1, 8.93, 6.71, 4.47, and 2.91 × 10⁻² M. Each curve is determined by 25–60 data points.

small volume of concentrated acetic acid in pyridine to a vigorously stirred, fully equilibrated solution of preformed pyCoO₂ (with additives as necessary) and measuring the gas evolved with time. The details are given in the Experimental Section.

The order of the reaction with respect to acetic acid was determined in the following manner. At constant initial concentration of pyCoO₂ the acetic acid concentration was varied from 6.8- to 37-fold excess. The raw data from each run were plotted as moles of oxygen evolved vs. time and are shown in Figure 1. The method of initial rates is prohibited because of the steepness of the curves near the origin as can be seen in Figure 1. Initial treatment of the data by other customary procedures, such as attempted fit to first- or second-order rate laws, indicated that kinetic behavior of unusual complexity was in operation. Therefore, the empirical rate law for dependence on acetic acid was determined by a different technique. The rate of the reaction (i.e., the slope of the moles of oxygen evolved vs. time curve) was measured for each run at various positions along the curve well away from the origin. Slopes were determined by hand or by fitting the data points of each run to a high-order polynomial expression and using the coefficients to calculate the derivative at each point desired.²⁸

At a given amount of oxygen evolved, the concentrations of all reactants and products are identical for each run except for the concentration of acetic acid, assuming no significant buildup of intermediates. This is true because the initial [pyCoO₂] is the same in each run and oxygen is maintained throughout each experiment at 1 atm pressure and is presumably in equilibrium at all times with the solution. Therefore, at equal moles of O₂ evolved the following equation can be used:

$$\text{rate} = \frac{-d[\text{pyCoO}_2]}{dt} \approx \frac{2 \times \text{rate of oxygen evolution}}{2} = k[\text{HOAc}]^n \quad (5)$$

Taking the logarithm of both sides:

$$\log(\text{rate}) = \log k + n \log [\text{HOAc}] \quad (6)$$

The order, *n*, is just the slope of a straight-line plot of log (rate) vs. log [HOAc].

The results of linear least-squares fit to eq 6 for several sets of data taken at different percent reactions in the range 22–81% are summarized in Table I. Excellent straight-line correlations were obtained for each series, which were verified by plots, and which were attested to by the high correlation coefficients (greater than 0.997 in all cases). The probability of obtaining such correlations from a parent population which is completely uncorrelated is less than 0.001.²⁹ It can be seen

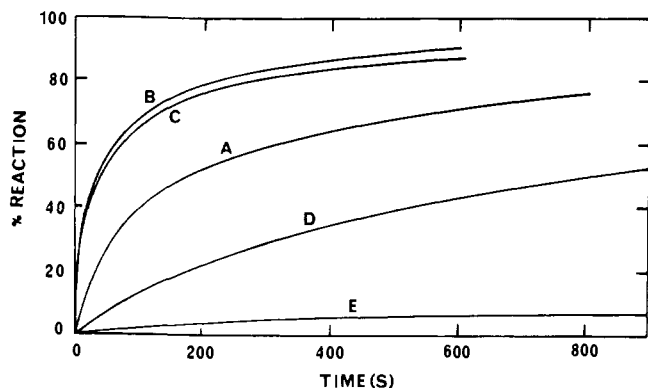


Figure 2. Effect of added salts on the rate of the reaction, $[\text{pyCoO}_2]_0 = 7.35 \times 10^{-3} \text{ M}$, $[\text{HOAc}]_0 = 8.66 \times 10^{-2} \text{ M}$: (A) no additives; (B) 5.1 equiv of $[\text{Co}^{\text{III}}\text{py}_2]\text{Br}$; (C) 4.9 equiv of $(n\text{-Bu})_4\text{NBr}$; (D) 3.3 equiv of $(n\text{-Bu})_4\text{NOAc}$; (E) 8.1 equiv of $(n\text{-Bu})_4\text{NOAc}$. Individual data points (approximately 40 for each run) are not shown.

that variation of $[\text{HOAc}]_0$ results in large changes in the rate as shown by the weighted average of $n = 2.39 \pm 0.05$. No trend of n with percent reaction was found, which is good evidence for a single mechanism operating.

The order with respect to pyCoO_2 was determined in a similar manner from runs in which $[\text{HOAc}]$ was held constant in large excess and $[\text{pyCoO}_2]$ was varied. At equal moles of oxygen evolved the concentrations of acetic acid and products will be identical for each run and therefore the determined rates and the known concentrations of the cobalt oxygen complex can be used to calculate the order n with respect to pyCoO_2 from equations exactly analogous to (5) and (6). This treatment, the results of which are shown in Table I, yields an average value of $n = 2.09 \pm 0.06$.

The order with respect to "product" was found by taking the rates at constant $[\text{pyCoO}_2]$ from the same runs which were used to determine the order in pyCoO_2 . The rate of each reaction was measured at a point on the reaction curve at which all runs have the same amount of oxygen gas remaining to be evolved. At these points $[\text{pyCoO}_2]$ is equal for all runs. The acetic acid, present initially in large excess and at the same concentration for each run, is in slightly different concentration at each of the points at which the rates are measured owing to differing amounts of product that have been formed. Because of the high observed order in acetic acid ($n = 2.39$) the effect of these small differences on the rate is significant. The use of equations similar to (5) and (6) but modified to take this into account³⁰ results in a value of n for "product" equal to -0.50 ± 0.04 (Table I). As with previous data for both HOAc and pyCoO_2 , the plots yield excellent correlation coefficients to a straight line and, furthermore, a value of n which is constant throughout the course of the reaction, strongly indicating that a single mechanism is in operation.

The above treatment for product is not dependent on which of the product species is responsible for the inhibition since all products are related stoichiometrically by a factor that merely becomes incorporated into the constant, k (see eq 5 and 6). The value of $n = -0.50$ means that the rate is inhibited by one-half order in product. Several experiments were carried out to determine the species responsible for inhibition. A tenfold increase in the hydrogen peroxide concentration (added as 30% aqueous solution) does not significantly affect the rate. In Figure 2 it is shown that the addition of 5.1 mol of $[\text{Co}^{\text{III}}\text{py}_2]\text{Br}$ or 4.9 mol of $(n\text{-C}_4\text{H}_9)_4\text{NBr}$ increases the rate by a factor of 4.5 and 4.4, respectively, at 50% reaction. The increase in rate is likely due to an increase in the concentration of pyridinium ion, $\text{C}_5\text{H}_5\text{N}^+\text{H}$, which is postulated to be in the rate-determining step (vide infra). The fact that both bromide salts cause nearly the same rate increase argues against any special effect

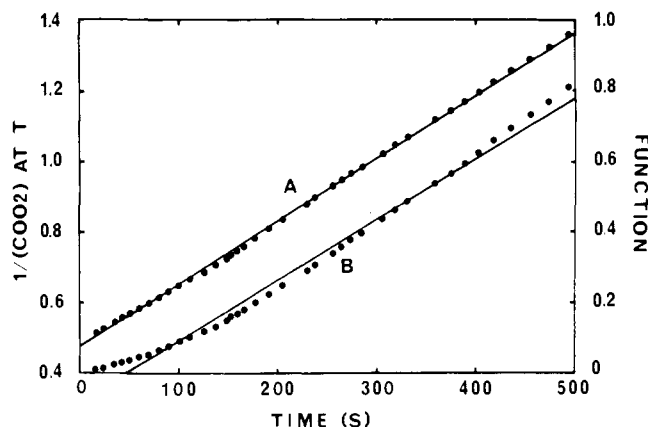


Figure 3. Fit of data for the reaction (to 65%) in the presence of tetra-*n*-butylammonium acetate to (A) a second-order plot according to eq 7a ($1/[\text{pyCoO}_2]$ at time t vs. time) and (B) second-order with inverse one-half order in product according to eq 8a (function vs. time). The ordinate scales are relative.

of the cobalt complex ion, $[\text{Co}^{\text{III}}\text{py}_2]^+$.

Addition of $(n\text{-C}_4\text{H}_9)_4\text{NOAc}$, on the other hand, causes a dramatic decrease in the rate (Figure 2). This suggests that acetate ion from $[\text{Co}^{\text{III}}\text{py}_2]\text{OAc}$ is the "product" responsible for inhibition. To test this, a run was carried out in the presence of a large excess of $(n\text{-C}_4\text{H}_9)_4\text{NOAc}$ and acetic acid (10.4 and 21.7 equiv, respectively). Equation 7 becomes the rate law if the dependence on product has been eliminated by the large excess of added acetate. Otherwise, eq 8 will be obeyed.

$$-\frac{d[\text{pyCoO}_2]}{dt} = k_{\text{obsd}}[\text{pyCoO}_2]^2 \quad (7)$$

$$\frac{1}{[\text{pyCoO}_2]} - \frac{1}{[\text{pyCoO}_2]_0} = k_{\text{obsd}}t \quad (7a)$$

$$-\frac{d[\text{pyCoO}_2]}{dt} = k_{\text{obsd}} \frac{[\text{pyCoO}_2]^2}{([\text{pyCoO}_2]_0 - [\text{pyCoO}_2])^{1/2}} \quad (8)$$

$$\frac{([\text{pyCoO}_2]_0 - [\text{pyCoO}_2])^{1/2} - \frac{1}{([\text{pyCoO}_2]_0)^{1/2}} \tanh^{-1} \left(\frac{[\text{pyCoO}_2]_0 - [\text{pyCoO}_2]}{[\text{pyCoO}_2]_0} \right)^{1/2}}{[\text{pyCoO}_2]} = k_{\text{obsd}}t \quad (8a)$$

A plot of $1/[\text{pyCoO}_2]$ vs. t according to the integrated form of eq 7 (eq 7a) yields a very good straight line to 87% reaction with an intercept within 2% of the actual value of $1/[\text{pyCoO}_2]_0$. An attempted fit to the integrated form of eq 8 (eq 8a, plot of the left-hand side vs. t) results in a very noticeably curved line. The two plots are shown in Figure 3.

The order with respect to oxygen was determined from 12 runs carried out at constant pressure of between 0.68 and 2.98 atm of oxygen. Acetic acid was present in large excess over pyCoO_2 . The data was analyzed in the following manner. The empirically determined orders in pyCoO_2 , $[\text{Co}^{\text{III}}\text{py}_2]\text{OAc}$, and HOAc and the known stoichiometry suggest the following approximate rate equation at constant pressure:

$$-\frac{dx}{dt} = k \frac{x^2(B - (A - x))^{5/2}}{(A - x)^{1/2}} \quad (9)$$

where $x = [\text{pyCoO}_2]$ at time t , $A =$ initial $[\text{pyCoO}_2]$, and $B =$ initial $[\text{HOAc}]$. The order in HOAc is approximated as 2.5. Rearrangement yields

$$-\int \frac{(A - x)^{1/2} dx}{x^2(B - A + x)^{5/2}} = kt \quad (10)$$

The solution of the indefinite integral on the left side of eq 10 is available.³¹ A plot of the resulting function of x vs. time for a given run will yield a straight line with a slope of k , if the relationship in eq 9 is obeyed. Incorporated in the rate constant then will be a term involving the concentration of oxygen.

Thus

$$k = k'[\text{O}_2]^n$$

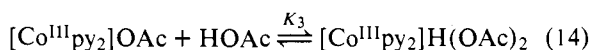
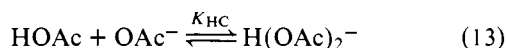
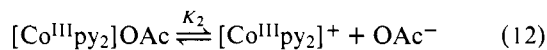
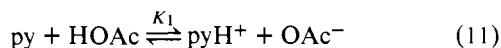
and the empirical order in O_2 , n , will be just the slope of a plot of $\log k$ vs. $\log P_{\text{O}_2}$, where P_{O_2} is the pressure in atmospheres of oxygen gas.

Use of eq 10 gives straight-line plots for each run to at least 75% reaction. Inclusion of the acetic acid term represents an improvement in the fit (acetic acid was present in 8.3-fold excess). It is significant that plots assuming other rate expressions using $[\text{HOAc}]$ as a constant, such as first order, second order, or first order with inverse half-order in product, do not even approach linearity. A plot³¹ of $\log k$ vs. $\log P_{\text{O}_2}$ is linear and yields a slope (order in O_2) of -1.12 . In addition, nine of the runs were done at the same initial $[\text{pyCoO}_2]$ and therefore a determination of n could be done in the same manner as with the other components, that is, by comparison of the measured rates at constant percent reaction. This gives an average value of -1.16 ± 0.04 for seven positions between 33 and 66% reaction.

The empirical rate law for this reaction is thus

$$-\frac{d[\text{pyCoO}_2]}{dt} = k_{\text{obsd}} \frac{[\text{pyCoO}_2]^{2.09} [\text{HOAc}]^{2.39}}{[\text{O}_2]^{1.12} [\text{Co}^{\text{III}}\text{py}_2\text{OAc}]^{0.50}}$$

C. Acid Species in the Mechanism. The evidence presented in this section will demonstrate the involvement of both undissociated acetic acid (HOAc) and free pyridinium ion (pyH^+) in the mechanism. The following equilibria are important with respect to free pyridinium ion in the reaction.



Acetic acid is known to be monomeric in pyridine.³² It is only very weakly dissociated because of the low dielectric constant of pyridine (12.3); values of 10.1³² and 12³³ have been measured for the $\text{p}K_{\text{a}}^{\text{py}}$ of acetic acid at 25 °C. Infrared evidence³⁸ has shown that weak carboxylic acids including acetic exist predominantly in the form of the hydrogen-bonded pyridine adduct ($\text{RCO}_2\text{H} \cdots \text{py}$) and not the undissociated ion pair ($\text{RCO}_2^-\text{pyH}^+$). With respect to eq 12 it is known that salts are only weakly dissociated in pyridine. The dissociation constants of alkylammonium and alkali metal salts of bromide, iodide, nitrate, picrate, acetate, and triphenylborofluoride ions at 25 °C are in the range $0.2\text{--}13.2 \times 10^{-4} \text{ M}^{-1}$.³⁵ The homoconjugation reactions of carboxylic acids shown in eq 13 and 14 for acetic acid and its conjugate anion are known to occur readily in aprotic solvents of low dielectric constant due to diminished solvation of acid and/or anion.³⁶

An expression for the concentration of pyridinium ion in the reaction solution can be derived by substitution of the equilibrium expressions in eq 11–14 into the equation of charge balance (Co^+ represents the complex ion, $\text{Co}^{\text{III}}\text{py}_2^+$):

$$[\text{pyH}^+] + [\text{Co}^+] = [\text{OAc}^-] + [\text{H}(\text{OAc})_2^-]$$

and by use of the stoichiometric relationship for total cobalt(III) product ($[\text{Co}^{\text{III}}]_{\text{T}}$) from the two forms in eq 14 that comprise bulk cobalt(III):

$$\begin{aligned} [\text{Co}^{\text{III}}]_{\text{T}} &= [\text{CoOAc}] + [\text{CoH}(\text{OAc})_2] \\ &= [\text{CoOAc}](1 + K_3[\text{HOAc}]) \end{aligned}$$

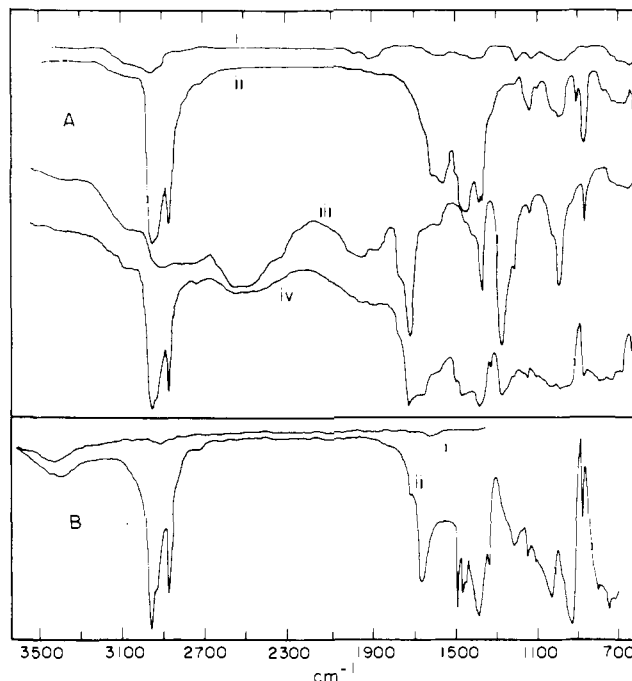


Figure 4. Infrared spectra in pyridine showing homoconjugative association between acetic acid and the salt tetra-*n*-butylammonium acetate at room temperature. (A) (i) Pyridine blank, (ii) 0.4 M $(n\text{-Bu})_4\text{NOAc}$, (iii) 0.4 M HOAc, (iv) 0.4 M $(n\text{-Bu})_4\text{NOAc} + 0.4$ M HOAc; (B) (i) KBr pellet blank, (ii) $(n\text{-Bu})_4\text{NH}(\text{OAc})_2$ in KBr.

This results in

$$[\text{pyH}^+] = \frac{K_1[\text{HOAc}](1 + K_{\text{HC}}[\text{HOAc}]^{1/2})}{\left(K_1[\text{HOAc}] + \frac{K_2[\text{Co}^{\text{III}}]_{\text{T}}}{1 + K_3[\text{HOAc}]}\right)^{1/2}} \quad (15)$$

The value of K_3 is sufficiently small (vide infra) so that $K_1[\text{HOAc}] \ll K_2[\text{Co}^{\text{III}}]_{\text{T}}/(1 + K_3[\text{HOAc}])$. Therefore, the final expression for $[\text{pyH}^+]$ becomes

$$\begin{aligned} [\text{pyH}^+] &= \frac{K_1[\text{HOAc}](1 + K_{\text{HC}}[\text{HOAc}]^{1/2})(1 + K_3[\text{HOAc}])^{1/2}}{(K_2[\text{Co}^{\text{III}}]_{\text{T}})^{1/2}} \quad (16) \end{aligned}$$

The experimentally determined order in acetic acid is 2.39. Depending on the values of K_{HC} and K_3 , eq 16 predicts an order with respect to HOAc of between 1 and 2 if the rate is first order in pyH^+ and between 2 and 3 if the rate is first order each in HOAc and pyH^+ . In either of these cases inverse half-order dependence on cobalt(III) product is expected, in agreement with experiment. For second-order dependence on pyH^+ , eq 16 predicts an order with respect to HOAc of between 2 and 4 depending on K_{HC} and K_3 but also predicts inverse *first-order* dependence on product, which is not consistent with observation. This argues for the involvement of both HOAc and pyH^+ .

The above reasoning is dependent on a demonstration that the homoconjugation equilibrium constants, K_{HC} and K_3 , agree with the observed order in acetic acid vis-à-vis eq 16. Evidence for the equilibrium corresponding to eq 14 for the salt tetra-*n*-butylammonium acetate at room temperature was obtained in this study by observing the changes in the infrared spectrum on addition of acetic acid. Figure 4A shows the spectra of 0.4 M $(n\text{-C}_4\text{H}_9)_4\text{NOAc}$, 0.4 M acetic acid, and an equimolar mixture (0.4 M each) in pyridine solution. The region between 2700 and 1800 cm^{-1} shows a decrease in intensity of the two O–H stretch absorptions of acetic acid³⁷ in the

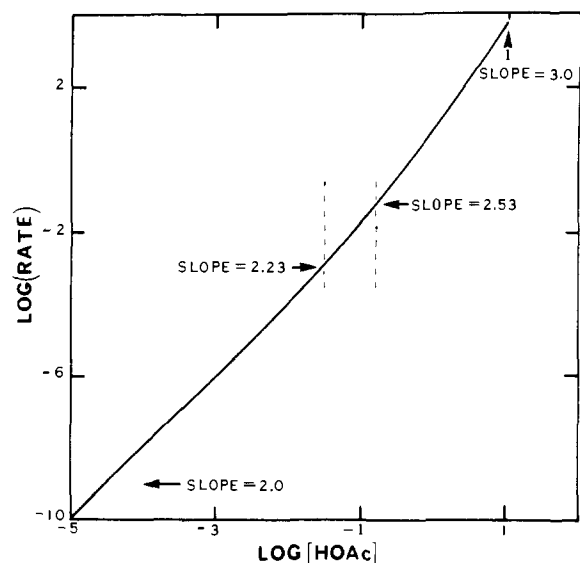


Figure 5. Plot of $\log(\text{rate})$ vs. $\log[\text{HOAc}]$ for a series of hypothetical runs in which $\log(\text{rate})$ is calculated according to eq 4] where $k_{\text{obsd}} = 1$, $K_{\text{HC}} = 15.75$, and $K_3 = 3.5$. The range of $[\text{HOAc}]$ actually used is between the dashed lines.

mixture as compared with the acid by itself. The mixture also shows the appearance of a new carbonyl absorption at about 1650 cm^{-1} and broad absorptions between 1200 and 1000 cm^{-1} and between 900 and 650 cm^{-1} that would not be present if the spectrum of the mixture were simply a composite of HOAc and the salt.

These changes can be attributed to formation of $(n\text{-C}_4\text{H}_9)_4\text{NH}(\text{OAc})_2$. Figure 4B shows an IR spectrum of tetra-*n*-butylammonium hydrogen diacetate (KBr pellet) that slowly crystallizes from concentrated solutions of acetic acid and tetra-*n*-butylammonium acetate in pyridine (satisfactory elemental analysis). This compound shows no discernible O-H stretch, a carbonyl stretch at 1665 cm^{-1} , and strong absorption between 1200 and 1000 cm^{-1} and between 900 and 650 cm^{-1} . It should be noted that this spectrum is similar to the published spectrum of sodium hydrogen diacetate.³⁸

The ν_{OH} at 2650 cm^{-1} for acetic acid can be used to calculate the equilibrium constant for $(n\text{-Bu})_4\text{NOAc}$ analogous to K_3 because the salts do not absorb in this region. A value of $13 \pm 3\text{ M}^{-1}$ was obtained. Determination of K_3 (eq 12) for $[\text{Co}^{\text{III}}\text{py}_2]\text{OAc}$ in a similar manner was not possible because the salts absorb significantly in this region. Qualitatively, however, the same changes occur in the IR spectrum. It is reasonable to expect the equilibrium constant for the cobalt(III) acetate salt to be similar to that for $(n\text{-Bu})_4\text{NOAc}$, since both compounds contain acetate ion situated next to a large cation with a single, buried positive charge.

The value of K_{HC} (eq 13) can in principle be obtained from solubility measurements of a suitable acetate salt as a function of acetic acid concentration³⁹ or by a potentiometric method.⁴⁰ The former method requires complete or nearly complete dissociation of the salts MOAc and $\text{MH}(\text{OAc})_2$ in solution,⁴¹ a condition which is not met in pyridine as judged from the reported dissociation constants of acetate salts of suitable solubility (Na^+ , Me_4N^+) and from the dissociation constants of salts of other anions,³⁵ which were considered in order to arrive at a reasonable estimate for $K_{\text{d}}^{\text{MH}(\text{OAc})_2}$ (see below). The latter method is based on the appearance in the potentiometric titration curve of a half-neutralization potential (hnp) at 50% titration with a strong base. The method is not applicable for $K_{\text{HC}} < 10^3$.⁴⁰ Van der Heijde has reported observing no hnp in the titration of acetic acid with alkylammonium hydroxide in pyridine,⁴² which indicates a K_{HC} of less than 10^3 .

A mechanism which includes both HOAc and pyH^+ yields the rate law in eq 17 at a constant $[\text{pyCoO}_2]$, $[\text{Co}^{\text{III}}]_{\text{T}}$, and $[\text{O}_2]$.

$$\text{rate} = k_{\text{obsd}}[\text{HOAc}]^2(1 + k_{\text{HC}}[\text{HOAc}])^{1/2} \times (1 + K_3[\text{HOAc}])^{1/2} \quad (17)$$

Taking the logarithm of each side gives

$$\log(\text{rate}) = \log k_{\text{obsd}} + 2 \log[\text{HOAc}] + \frac{1}{2} \log(1 + K_{\text{HC}}[\text{HOAc}]) + \frac{1}{2} \log(1 + K_3[\text{HOAc}]) \quad (18)$$

By knowing K_{HC} and K_3 , a plot of $\log(\text{rate})$ vs. $2 \log[\text{HOAc}] + \frac{1}{2} \log(1 + K_{\text{HC}}[\text{HOAc}]) + \frac{1}{2} \log(1 + K_3[\text{HOAc}])$ should yield a straight line with a slope of 1.0. However, since the values of both constants are unavailable, it is imperative to determine whether a reasonable range of values for K_{HC} and K_3 will fit the expression in eq 18. This was done in the following manner. It can readily be shown that

$$K_{\text{HC}} = \frac{K_{\text{d}}^{\text{CoH}(\text{OAc})_2}}{K_{\text{d}}^{\text{CoOAc}}} K_3 \quad (19)$$

where $K_{\text{d}}^{\text{CoH}(\text{OAc})_2}$ and $K_{\text{d}}^{\text{CoOAc}}$ are the dissociation constants of the respective $[\text{Co}^{\text{III}}\text{py}_2]^+$ salts and K_3 is the equilibrium constant for eq 14.

The ratio of dissociation constants in eq 19 is expected to be greater than 1.0 because of greater charge delocalization in (enhanced stability of) the hydrogen diacetate ion as compared with acetate ion. Furthermore, it is intuitively reasonable that $K_{\text{HC}} > K_3$ because hydrogen bonding of acetic acid to free acetate ion would be expected to be more favorable than to acetate of an ion pair that is already partially stabilized by being situated next to a positive ion. The ratios $K_{\text{d}}^{\text{MX}}/K_{\text{d}}^{\text{MOAc}}$ for $\text{M} = (n\text{-Bu})_4\text{N}^+$ and various anions X in pyridine at 25°C by conductance measurements³⁹ follow: BFPh_3^- , 7.8; picrate, 7.5; I^- , 2.4; NO_3^- , 2.2; Br^- , 1.5. Although it is not possible to predict the value for $\text{X} = \text{H}(\text{OAc})_2^-$, it is likely to fall in this range (1.5–7.8). The same ratios should apply to the salts of the cobalt(III) complex ion since the dissociation constants of a series of salts with the same cation depend only on relative solvation of the anion. In addition, temperature effects on these values should be minimal.

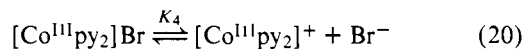
Accordingly, a program was designed to fit the rate data to eq 18 where eq 19 was substituted for K_{HC} . The ratio $K_{\text{d}}^{\text{CoH}(\text{OAc})_2}/K_{\text{d}}^{\text{CoOAc}}$ was varied from 1.5 to 7.7 by increments of 0.2 and the values of K_3 which resulted in the slope of $\log(\text{rate})$ vs. $2 \log[\text{HOAc}] + \frac{1}{2} \log(1 + K_{\text{HC}}[\text{HOAc}]) + \frac{1}{2} \log(1 + K_3[\text{HOAc}])$ equal to 1.00 ± 0.01 were taken. K_3 is found to vary from 2.5 to 6.4 M^{-1} (averages from nine sets of data; standard deviation $\pm 40\%$), which is in reasonable agreement with the experimentally determined value of 13 M^{-1} for $(n\text{-Bu})_4\text{NOAc}$ at room temperature.

It may be argued that if eq 17 is obeyed curvature should have been observed in the plots of $\log(\text{rate})$ vs. $\log[\text{HOAc}]$ in which the value of $n = 2.39$ was obtained, whereas good straight lines were found. This is not necessarily so. In Figure 5 is shown a plot of $\log(\text{rate})$ vs. $\log[\text{HOAc}]$ for hypothetical runs in which $\log(\text{rate})$ is calculated according to eq 18 with $k_{\text{obsd}} = 1$, and $K_{\text{d}}^{\text{CoH}(\text{OAc})_2}/K_{\text{d}}^{\text{CoOAc}}$ and K_3 assuming the values 4.5 and 3.5, respectively, which are the midpoint values of the above analysis. The slope changes from 2.0 to 3.0 in the concentration range 10^{-4} – 10 M and it would be difficult indeed to observe curvature in the range of concentration actually used (2.9 – $15.6 \times 10^{-2}\text{ M}$) with normal experimental scatter of points. In fact, the slope in this range changes only from 2.23 to 2.53.

Conceptually, a change in the properties of the solvent with varying acetic acid concentration could be responsible for the abnormal dependency on acetic acid (i.e., 2.39 vs. 2.0 or 3.0). Dielectric constant or solvent polarity changes could affect the

energy of the transition state or alter one or more of the equilibrium constants involved in the rate law. However, both the dielectric constant⁴³ and the solvent-polarity parameter, Z ,⁴⁴ change very little in the range of acid concentration used and are not likely to significantly affect the rate.⁴⁵

Additional experimental evidence supports the involvement of pyH^+ . As described previously, addition of $[\text{Co}^{\text{III}}\text{py}_2]\text{Br}$ causes an increase in the rate. By including the equation

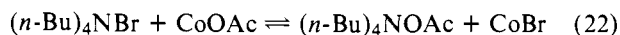


along with the equilibria in eq 11–14 it can be seen qualitatively that this result is expected because an increase in the concentration of free cobalt ion will reduce free acetate ion in solution, which in turn will result in an increase in the pyridinium ion concentration. The following expression can be derived for the ratio of the concentrations of pyridinium ion with (w) and without (w/o) added $[\text{Co}^{\text{III}}\text{py}_2]\text{Br}$ (CoBr represents the added salt and $[\text{Co}]_{\text{prod}}$ represents the total concentration of product which is partitioned between CoOAc and $\text{CoH}(\text{OAc})_2$):

$$\frac{[\text{pyH}^+]_w}{[\text{pyH}^+]_{w/o}} = \frac{\left(1 + K_{\text{HC}}[\text{HOAc}] + \frac{K_4[\text{CoBr}]}{K_2[\text{Co}]_{\text{prod}}} (1 + K_3[\text{HOAc}])\right)^{1/2}}{(1 + K_{\text{HC}}[\text{HOAc}])^{1/2}} \quad (21)$$

This expression is valid for comparison of runs at the same initial $[\text{HOAc}]$ and at equal $[\text{Co}]_{\text{prod}}$ (i.e., equal percent reaction) and if the assumption is made that the equilibrium constants K_1 , K_2 , K_{HC} , and K_3 are not significantly altered by the increase in ionic strength accompanying the addition of CoBr. This equation does indeed predict an increase in rate, if the rate is dependent on $[\text{pyH}^+]$, by an amount which is a function of $[\text{CoBr}]$. For two runs carried out at the same initial concentrations of starting materials, the reaction curves of which are shown in Figure 2, eq 21 predicts a rate ratio of 2.8–3.7 at 50% reaction, depending on what values of K_{HC} and K_3 are used from the data obtained by the fit to eq 18 as described above, if the rate law is first order in pyH^+ .⁴⁶ The experimentally determined ratio is 4.5. Equation 21 also predicts that the rate ratio will decrease with increasing percent reaction (i.e., increasing $[\text{Co}^{\text{III}}]_{\text{T}}$). This is verified by the same experiments; the rate ratio decreases smoothly from 4.7 at 40% reaction to 2.7 at 80%.

The addition of tetra-*n*-butylammonium bromide has also been shown to increase the rate (Figure 2). In the presence of this salt the following ion exchange reaction with the product can occur:



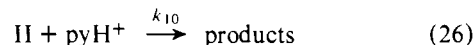
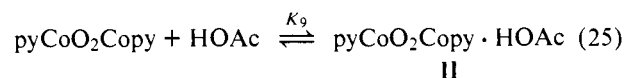
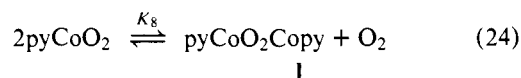
Consideration of the equilibria in eq 11–14, 20, and 22 and the dissociation equilibria for $(n\text{-Bu})_4\text{NBr}$ (K_5) and $(n\text{-Bu})_4\text{NOAc}$ (K_6) as well as the homoconjugation equilibrium for $(n\text{-Bu})_4\text{NOAc}$ (K_7 , analogous to K_3) leads to the following expression for the concentration of pyridinium ion in the presence of the added alkylammonium salt:

$$[\text{pyH}^+] = K_1[\text{HOAc}] \times \left(\frac{1 + K_{\text{HC}}[\text{HOAc}] + \frac{K_4x}{K_2([\text{Co}]_{\text{prod}} - x)} (1 + K_3[\text{HOAc}])}{K_1[\text{HOAc}] + \frac{K_2([\text{Co}]_{\text{prod}} - x)}{1 + K_3[\text{HOAc}]} + \frac{K_6x}{1 + K_7[\text{HOAc}]}} \right)^{1/2} \quad (23)$$

where $x = [\text{CoBr}]$ from the ion exchange reaction (eq 22). In the absence of added $(n\text{-Bu})_4\text{NBr}$ the expression for $[\text{pyH}^+]$

is given by eq 15. If the ion exchange reaction (eq 22) is small or very slow, then x will approach zero and eq 23 becomes identical with eq 15 and no effect on the rate by added alkylammonium bromide will be observed. If the ion exchange is appreciable (there is no reason to expect the contrary) the numerator of eq 23 will be greater than that of eq 15 for all x . Furthermore, the denominator of eq 23 will be less than that of eq 15 for all x assuming that (1) the homoconjugation constants for CoOAc (K_3) and $(n\text{-Bu})_4\text{NOAc}$ (K_7) are approximately equal, which is valid since acetate ion is in a similar environment with both cations, and (2) the dissociation constant for CoOAc (K_2) is greater than that of $(n\text{-Bu})_4\text{NOAc}$ (K_6), which is a valid assumption because the cobalt complex cation is expected to be better solvated than $(n\text{-Bu})_4\text{N}^+$. Thus, for any degree of ion exchange in eq 22, the concentration of pyH^+ , and therefore the rate, will increase.

D. Mechanism. The following mechanism is consistent with all the experimental data:



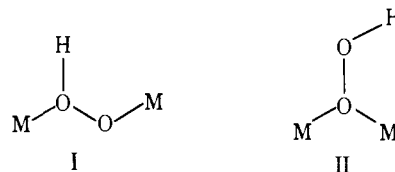
Note that eq 26 contains free, *dissociated* pyH^+ , and of course this is very important.

The derived rate expression, assuming that eq 24 and 25 are fast and reversible and eq 26 is rate limiting and irreversible, is

$$-\frac{d[\text{pyCoO}_2]}{dt} = \frac{2d[\text{O}_2]}{dt} = \frac{k_{10}K_8K_9[\text{pyCoO}_2]^2[\text{HOAc}][\text{pyH}^+]}{[\text{O}_2]} \quad (27)$$

The orders with respect to pyCoO_2 and O_2 predicted by this sequence of reactions agree well with the experimentally determined values (2.09 and -1.12 , respectively). The observed dependencies on acetic acid (2.39 order) and cobalt(III) acetate product (-0.50 order) together with the observed effect of acetate and bromide salts on the rate and the demonstrated homoconjugation equilibria accommodate a scheme that is first order each in acetic acid and free pyridinium ion, as outlined in the previous section.

The intermediate I is a binuclear μ -peroxy complex. This species is often the predominant product in the reaction of oxygen with cobalt(II) complexes of suitable ligands, especially



in aqueous solution. The metal is considered to be formally in the 3+ oxidation state bound to a formally reduced O_2 ligand of peroxide nature (O_2^{2-}), although the extent of charge transfer from the cobalt to the dioxygen probably varies with the field strength of the other ligands on the metal.⁴⁷ N,N' -Ethylenebis(acetylacetonimate) is considered to be a ligand of strong field strength and pyridine of moderate strength.⁴⁸

The reactions of many cobalt complexes with oxygen leading to the μ -peroxy species have been extensively studied⁴⁷ and the overwhelming evidence indicates that they proceed by coupling of an initial mononuclear oxygen complex with an unoxxygen-

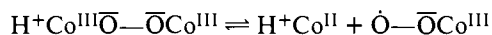
ated cobalt(II) complex as shown in eq 28 and 29.



For the cobalt complex used in this study as well as others the oxygenation stops at the mononuclear complex stage (eq 28) and the binuclear complex is thermodynamically unstable with respect to it. Since eq 28 and 29 have been shown to be reversible for many other systems, it is likely that the binuclear μ -peroxy species I exists in small concentrations in the reaction mixture in equilibrium with pyCoO_2 by way of these steps.

Also, it is important to note that the available evidence indicates that the concentration of intermediates must be small. Addition of acetic acid to a pyridine solution of the complex pyCoO_2 causes a smooth change in its electronic spectrum to the product cobalt(III) complex. Furthermore, ESR spectra during the reaction show only the unaltered signal for the oxygen complex.

The kinetic results indicate that both acids are involved in the mechanism but one cannot distinguish which is involved in eq 25 and which in eq 26. The species II is proposed to be a μ -peroxy complex that is either hydrogen bonded to or protonated with a molecule of acid, and which then reacts with a molecule of the other acid to yield free hydrogen peroxide and oxidized metal. The site of protonation (or hydrogen bonding) may be either the peroxy bridge or the oxygen or nitrogen atoms of the equatorial ligand on one of the cobalt atoms. The latter situation would have the effect of reducing the stability of Co(III) relative to Co(II) by reducing the field strength of the ligand and would be expected to cause a simultaneous demand for electrons from the peroxide bridge. The O_2 bridge would then become less basic and also less able to dissociate from the metal as peroxide. In the extreme, this would result in an intramolecular electron transfer leading to dissociation to a protonated cobalt(II) complex and the mononuclear oxygen species as shown below for the generalized case.



Protonation of the equatorial ligand therefore is probably a nonproductive pathway with respect to the formation of H_2O_2 and cobalt(III).

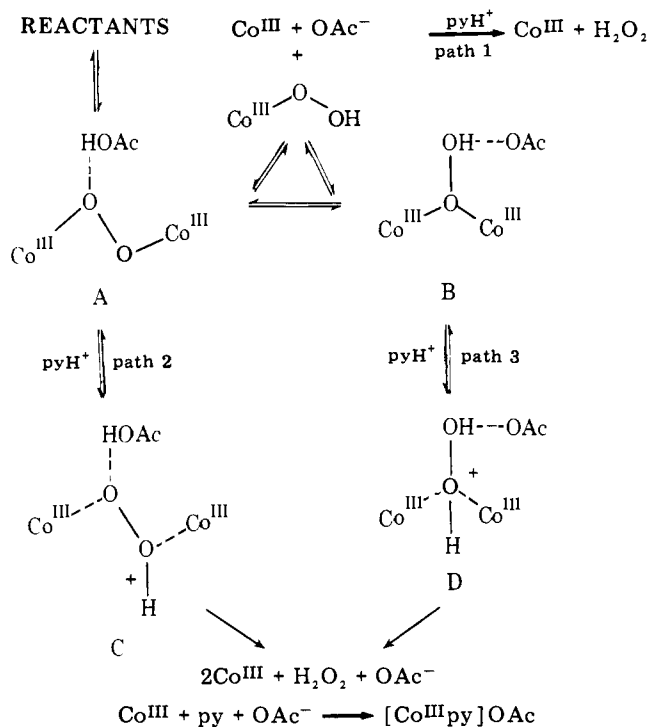
Protonation on the peroxide bridge would also tend to destabilize the 3+ oxidation state of the metal adjacent to the oxygen atom that is protonated, but intramolecular electron transfer to cobalt would now be disfavored because of the diminished reduction potential of the peroxide bridge due to the electrophilicity of the proton. The O_2 ligand is now better disposed toward dissociation as free H_2O_2 in a subsequent step.

Several protonated binuclear μ -peroxy cobalt compounds have been reported. The structures have been proposed to be either of the type I⁴⁹ or the rearranged type II^{11a,c,49a,b,50,51} and are based mainly on comparison of their properties with those of the parent μ -peroxy complex except for DL-[(en)₂-Co(O₂H)(NH₂)Co(en)₂](NO₃)₄·2H₂O, the structure of which has been determined by X-ray crystallography to be of the type II.⁵⁰ Interestingly, reversion to the cobalt(II) complex and oxygen on acidification occurs for all except the cyano^{49c} and dipeptide dianion^{11a,c} complexes, which are reported to yield hydrogen peroxide and cobalt(III) species.

Protonation and dissociation of peroxide from a peroxo-bridged dicobalt complex is the mechanism which is most likely to be in operation in the present reaction. The possible detailed mechanisms are outlined in Scheme I. Path 1 involves the intermediacy of a mononuclear hydroperoxy species and is similar to the mechanism proposed for reaction of μ -peroxybis(pentacyanocobaltate(III)) with acid.^{49c,52} It can be ruled out here because it requires either (1) a first-order rate law in

Scheme I

(Co^{III} represents the complex [(Co^{III})py]⁺)



acetic acid (or pyH^+) if formation of the hydroperoxy intermediate from A or B is rate limiting or (2) inhibition by cobalt(III) ion if decomposition of the intermediate to hydrogen peroxide is taken as the rate-limiting step.

Paths 2 and 3 proceed through the diprotonated intermediates, C and D, respectively. Both structures C and D are sterically accessible (as well as the monoprotated species A and B and their unprotonated precursors) according to space-filling molecular models. However, for D and its precursors the Co-O-Co bond angle must be greater than about 110° and the Co-O bond length greater than or equal to about 2.0 Å because of steric repulsions between the equatorial ligand systems on each cobalt atom. These dimensions can be compared with the bond angle of 102° and bond length of 1.92 Å for the analogous compound DL-[(en)₂Co(O₂H)(NH₂)Co(en)₂](NO₃)₄·2H₂O.⁵⁰ It is not known how far these dimensions can be stretched and still maintain stability.

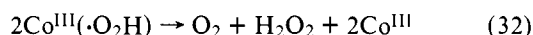
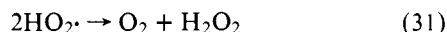
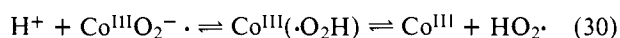
Any mechanism must rationalize the involvement of both acids. Path 3 affords a reasonable explanation. In the unprotonated form of species B the terminal oxygen is likely to be far more basic than the bridging oxygen. It is well known that bridging amido and hydroxo groups are weak Brønsted bases because of the decreased energy and number of available electron pairs. The hydroperoxy group in the analogous compound DL-[(en)₂Co(O₂H)(NH₂)Co(en)₂]⁴⁺ has a $\text{p}K_{\text{a}}^{\text{aq}} = 11.49\text{a}.$ ⁵⁰ If the $\text{p}K_{\text{a}}^{\text{aq}}$ of B is similar, $\Delta\text{p}K_{\text{a}}$ between it and acetic acid is about 6, assuming that $\Delta\text{p}K_{\text{a}}$ is the same in pyridine as in water. This makes the unprotonated form of B a strong base with respect to both HOAc and pyH^+ and protonation will be close to the limits of diffusion with either acid. Therefore, the conjugate base of B will be *general* acid protonated. Because acetic acid is in much larger concentration than pyH^+ (typically, 10^{-1} vs. 10^{-8} M), B will be an adduct of acetic acid. Protonation of the second oxygen, on the other hand, will require strong acid because of its much lower basicity. Protonation will serve to weaken the cobalt-oxygen bond and result in dissociation.

The involvement of both acids in path 2 can be explained by invoking a sufficiently large equilibrium constant for formation

of the acetic acid adduct A (K_9 , eq 25), such that the bulk of the μ -peroxo species in solution is present in this form, and by supposing that strong acid is necessary to sufficiently weaken the Co–O bond (i.e., full protonation rather than the hydrogen-bonded situation depicted in A). A large equilibrium constant for formation of A is not unreasonable. The μ -peroxo species need only be somewhat more basic than the solvent pyridine ($pK_a^{aq} = 5$). The pK_a^{aq} 's of the conjugate acids of other complexes vary from 0.8 for the highly positively charged $[(en)_2Co(O_2)(NH_2)Co(en)_2]^{3+}$ ^{49a} to 12 for the highly negatively charged $[(CN)_5CoO_2Co(CN)_5]^{6-}$ ^{49c} the μ -peroxo complex in this study is neutral. The pK_a in Me_2SO for the conjugate acid of another neutral μ -peroxo complex, $[Co_2(salen)_2]O_2$, has been reported to be 5.5.⁵³ Furthermore, the depiction of A as a hydrogen-bonded adduct is reasonable because of the reluctance of the solvent to support charge-separated species, as long as the ΔpK_a^{aq} of A and acetic acid is less than about 3.5, as has been shown for 1:1 pyridine–acid complexes in pyridine.^{34b}

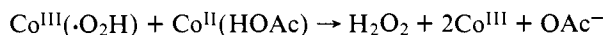
A clear choice between paths 2 and 3 cannot be made at this time.

E. Other Mechanistic Considerations. Alternative pathways involving hydroperoxyl radical intermediates either in free or complexed form have also been considered (eq 30–32). The complexed form $Co^{III}(\cdot O_2H)$ can result from protonation of the superoxide-like dioxygen ligand in the mononuclear oxygen complex.



Dissociation of this species would give rise to the free hydroperoxyl radical (eq 30). Short-lived hydroperoxyl radicals complexes analogous to $Co^{III}(\cdot O_2H)$ are known for transition metals in high oxidation states including Cu(II), Ti(IV), Zr(IV), Ce(III), and Mo(VI) that have been observed by ESR upon mixing of the metal ion with photolytically or chemically generated $HO_2\cdot$ in a flow system.⁵⁴ The equilibrium constants for $M + HO_2\cdot \rightleftharpoons M(HO_2\cdot)$ are generally high ($>10^3 M^{-1}$). Both free and complexed $HO_2\cdot$ decompose by disproportionation to give oxygen and hydrogen peroxide (eq 31 and 32).

Although the mechanisms in eq 30–32 disagree with the kinetic results (especially in their lack of dependence on $[O_2]$), the following oxidation–reduction as the rate limiting step would be consistent with the kinetic data.

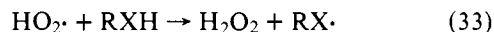


$Co^{II}(HOAc)$ represents some molecular adduct of the cobalt(II) complex with acetic acid. The above mechanism can be considered viable only if both species on the left-hand side are reversibly formed from their respective constituents.

No ESR signals attributable to either hydroperoxyl radical or its cobalt complex were observed in this work. Frozen spectra (90 K) of pyridine solutions of $pyCoO_2$ to which either acetic or *p*-toluenesulfonic acid was added show only the presence of unreacted starting complex, the signal⁵⁵ of which decays progressively to zero after several cycles of freeze–thaw. Frozen dimethylformamide solutions containing 2 equiv of pyridine to which strong acid had been added typically showed no signal because the reaction is very fast, unless the sample was frozen simultaneous with acid injection, and then only the signal for $BCoO_2$ ($B = py$ or DMF) was present.

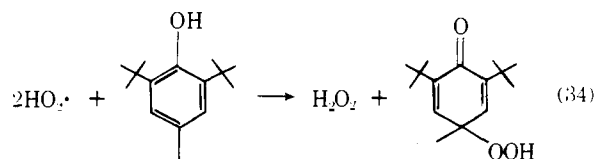
Experiments were performed to detect radical intermediates by carrying out the reaction in the presence of compounds containing easily abstractable hydrogens including hydroquinone, 2,4,6-tri-*tert*-butylphenol, thiophenol, and *N,N'*-diphenyl-*p*-phenylenediamine. These compounds are easily

oxidized by reactive radicals in a hydrogen-abstraction step,⁵⁶ which for the hydroperoxyl radical would be shown in the equation



It was expected that the supposed intermediate $HO_2\cdot$ or $Co^{III}(\cdot O_2H)$ would be diverted from its normal disproportionation (eq 31 or 32) and react with the scavenger according to eq 33 to produce more hydrogen peroxide at the expense of oxygen. This was indeed found to be the case. However, subsequent investigation revealed the probable occurrence of reaction between the scavenger and $pyCoO_2$ itself. While this work was in progress others⁵⁷ reported similar reactions and a mechanism. Our results are in accord with theirs.

Other experiments failed to detect radical intermediates. The reaction of $pyCoO_2$ with acetic acid fails to initiate any detectable autoxidation of cumene to cumene hydroperoxide when carried out in the presence of 40-fold excess of cumene. Finally, an experiment was performed which would seem to rule out the involvement of the hydroperoxyl radical, at least. 2,6-Di-*tert*-butyl-4-methylphenol is reported⁵⁸ to react with $HO_2\cdot$ to yield a stable hydroperoxydienone (eq 34). When a



solution of $pyCoO_2$ at 0 °C in pyridine was added dropwise to a solution of 10 equiv of the phenol in 50% acetic acid in pyridine (to maximize the rate so as to minimize reaction of $pyCoO_2$ with the phenol) and the resulting solution analyzed by TLC, none of the hydroperoxide nor its corresponding alcohol (which could be formed by metal ion catalyzed decomposition of the hydroperoxide) was formed—the limits of detection as determined with authentic samples being <1% yield based on reaction 34.

F. Conclusion. The kinetic experiments on this reaction show second-order behavior in the cobalt oxygen complex and inverse first-order behavior in oxygen concentration. This implies the involvement in the transition state of one molecule of $pyCoO_2$ and one molecule of $pyCo^{II}$ which has resulted from dissociation of $pyCoO_2$ according to eq 28. The kinetic analysis also demonstrates the participation of both acetic and dissoiated pyridinium acids.

The results indicate an intermediate binuclear μ -peroxo complex for this reaction and that superoxide or hydroperoxyl radicals are not produced as discrete reaction entities. This may be a common phenomenon for transition-metal complexes. The superoxide path has been proposed by investigators who observed first-order dependence on both metal and O_2 . Examples include Fe^{2+} in acidic solution in the presence of various ligands,² Cu^+ in aqueous solution,³ $V^{III}(salen)^+$ and V^{3+} in perchloric acid solution,⁴ and Ti^{3+} in acidic solution.⁵ Earlier workers proposed a direct electron transfer to dioxygen. A strong reason for invoking metal oxygen complexes in these mechanisms then arose after it was observed that under certain conditions the kinetics displayed second-order or mixed first- and second-order behavior in metal, and after numerous oxygen adducts were discovered. Thus it is possible that in many cases that have been assigned the superoxide mechanism the observed first-order kinetics in metal may just be a limiting case of the binuclear path (eq 3) with formation of $M-O_2$ as the rate-determining step. (This has apparently been ruled out in one specific case of a Cu(I) complex.^{3a}) It may therefore be desirable to reexamine these systems, especially in view of the fact that $O_2^{\cdot-}(HO_2\cdot)$ has not been directly observed.

The preference for the binuclear pathway for the cobalt

complex of this study may simply be a reflection of the relatively high stability constant of $M^+-O_2^-$ or $M^+-\dot{O}_2H$ as compared with the rate of further oxidation of another metal by $O_2^-(HO_2)$ vis-à-vis eq 2. The dissociation constant of a cobalt(II) porphyrin dioxygen complex to superoxide and cobalt(III) ions has been estimated to be less than $10^{-12} M^{-1}$.⁵⁹ Furthermore, $M^+-\dot{O}_2H$ must be relatively slow to disproportionate according to eq 32, in contrast with hydroperoxyl radical complexes of some other transition-metal ions (see section E), or else $M^+-\dot{O}_2H$ is present in concentrations too small for eq 32 to compete with the binuclear path (i.e., $M-O_2$ may be a weak base).

An $O_2^-(HO_2)$ generating mechanism is viable in cases where formation of $M-O-O-M$ is prohibited for steric reasons. Hemoglobin with its isolated porphyrin systems has been found to oxidize by way of a "proton-assisted nucleophilic displacement" of dioxygen by anions in the medium,⁶⁰ a mechanism that is closely related to eq 2. In addition is the observation that bulky ferroporphyrins designed to prevent close approach of two molecules are able to withstand irreversible autoxidation.⁶¹ In light of this it would be of interest to study the autoxidation of cobalamin, the Co(II) derivative of vitamin B₁₂, which is also sterically unable to form the binuclear μ -peroxo complex.

Experimental Section

N,N'-Ethylenebis(acetylacetoniminato)cobalt(II) was prepared under inert atmosphere according to Everett and Holm⁶² from *N,N'*-ethylenebis(acetylacetonimine),⁶³ bis(tetraethylammonium)tetrabromocobaltate(II),⁶⁴ and potassium *tert*-butoxide in *tert*-butyl alcohol. One recrystallization from 3:1 toluene-heptane under inert atmosphere gave pure material. Anal. (C₁₂H₁₈CoN₂O₅) C, H, N. The compound can be handled in air for short periods but must be stored in a dry, inert atmosphere.

Dipyridine-*N,N'*-ethylenebis(acetylacetoniminato)cobalt(III) bromide was made according to Costa et al.²⁴ The corresponding acetate monohydrate salt was made in the same manner except that the reaction was carried out at room temperature. The viscous, dark brown oil remaining after evaporation of the solvent was taken up in CHCl₃ and washed with 30% (w/v) aqueous sodium acetate. Two recrystallizations from pyridine followed by drying under vacuum at room temperature yielded brown crystals (mp 115–126 °C dec with evolution of pyridine). Anal. (C₂₂H₃₃CoN₄O₅) C, H, N. UV-vis: λ_{max} (log ϵ) 341 nm (3.86), 451 (2.88) in pyridine, identical with that of the bromide salt. NMR in pyridine and in D₂O was identical with those of the bromide salt except for the presence of the acetate methyl protons at δ 2.4 and water protons. Tetra-*n*-butylammonium acetate was prepared by metathesis of tetra-*n*-butylammonium iodide and silver acetate in anhydrous methanol (distilled from Mg) and dried at 90 °C under vacuum for 24 h. The IR spectrum (Nujol) showed the absence of water. It was stored and handled under a dry atmosphere. *N,N'*-Diphenyl-*p*-phenylenediamine, 2,4,6-tri-*tert*-butylphenol, thiophenol, and hydroquinone were purchased commercially and recrystallized or distilled before use. 2,6-Di-*tert*-butyl-4-hydroperoxy-4-methylcyclohexa-2,5-dienone and the corresponding 4-hydroxy compound were prepared according to Kharasch and Joshi.⁶⁵

Reagent grade pyridine was distilled from BaO. Reagent grade dimethylformamide was distilled from P₂O₅ at reduced pressure. Toluene and heptane were distilled from sodium. Acetic acid was purified by distillation from CrO₃ followed by distillation from B(O₂CCH₃)₃. Cumene was purified by first extracting the hydroperoxide impurity with 2% NaOH solution followed by washing with concentrated H₂SO₄ (caution!), water, dilute NaHCO₃, and finally water. The solvent was then distilled from and stored over sodium. All solvents were stored under nitrogen or argon. Oxygen gas (99.995%) was purchased from Matheson and used without further purification.

All gas-measurement experiments were carried out at constant pressure of oxygen in a doubly jacketed apparatus consisting of a reaction flask connected to one of two identical graduated burets that were set up parallel to each other and in a vertical position. Manometer fluid from a common external reservoir to the two burets allowed for

equalization of pressure between the buret connected to the reaction flask and the other buret that was connected to a source of gas at known pressure. A nonviscous, nonvolatile organic solvent (2-methoxyethanol or decalin) was used as the manometer fluid, which allowed very small differences in pressure between the two burets to be detected. Fluid from a constant-temperature bath was pumped through the inner jacket. The outer jacket was evacuated to provide insulation.

Prior to the experiment, the solvent along with necessary additives was placed in the flask and stirred vigorously while oxygen was passed through the apparatus to purge it of other gases and saturate the solvent with oxygen. The solvent was then allowed to equilibrate with the gas at known pressure for a sufficient length of time. A small volume of a freshly prepared, oxygen-free solution of Co^{II}acacen was injected into the reaction flask by means of a calibrated syringe through a leak-proof septum fitting above the flask and the volume of gas taken up at constant pressure was measured after reequilibration. The kinetics were run by injecting a small volume of standardized 5.2 M acetic acid in pyridine to the fully equilibrated solution of pyCoO₂ and measuring the evolution of gas at constant pressure (i.e., while maintaining equal manometer fluid levels in each buret). Proper blanks were run to correct for oxygen solubility and the change in volume due to temperature of the injected solutions. Gas solubility data⁶⁶ show that the dissolved inert gas from the injected solutions (nitrogen or argon) only insignificantly changed the partial pressure of oxygen in the system. The solubility of oxygen in 8.6×10^{-2} M acetic acid in pyridine was determined in the same apparatus by injecting known volumes (about 4 mL) of solution withdrawn by syringe from the bottom of an 18-cm column of solution (about 45 mL) in a thick-walled glass tube that had been degassed by several freeze-pump-thaw cycles and opened to air just prior to use. The solubility of oxygen was found to follow Henry's law. ESR spectra were recorded on a Varian 4502 spectrometer operating at 9.5 GHz (X band).

Acknowledgment. This work was supported by the National Institutes of Health, Grant GM-15373. The authors wish to thank Professor F. Ann Walker, San Francisco State University, for assistance in running the ESR experiments.

Supplementary Material Available: Solution of the indefinite integral in eq 10 and logarithmic plot of the rate constant determined according to eq 10 vs. P_{O_2} (5 pages). Ordering information is given on any current masthead page.

References and Notes

- D. Behar, G. Czapski, J. Rabani, L. M. Dorfman, and H. A. Schwarz, *J. Phys. Chem.*, **74**, 3209 (1970).
- A. D. Gilmour and A. McAuley, *J. Chem. Soc. A*, 1006 (1970); M. Cher and N. Davidson, *J. Am. Chem. Soc.*, **77**, 793 (1955); Y. Kurimura and H. Kuriyama, *Bull. Chem. Soc. Jpn.*, **42**, 2239 (1969); Y. Unno and G. Wada, *ibid.*, **46**, 1188 (1973).
- (a) R. D. Gray, *J. Am. Chem. Soc.*, **91**, 56 (1969); (b) J. S. Valentine and A. B. Curtis, *ibid.*, **97**, 224 (1975); (c) D. V. Sokol'skii, Y. A. Dorfman, and L. S. Ernestova, *Zh. Fiz. Khim.*, **46**, 1855 (1972); (d) T. Yano, T. Suetaka, and T. Umehara, *Nippon Kagaku Kaishi*, **11**, 2194 (1972); *Chem. Abstr.*, **78**, 34391d (1973).
- J. B. Ramsey, R. Sugimoto, and H. J. DeVorkin, *J. Am. Chem. Soc.*, **63**, 3480 (1941).
- D. P. Feld'man and B. P. Matseevskii, *Russ. J. Phys. Chem. (Engl. Transl.)*, **47**, 1291 (1973); H. A. Mackenzie and F. C. Tompkins, *Trans. Faraday Soc.*, **38**, 465 (1942).
- J. A. Arce, E. Spodine, and W. Zamudio, *J. Inorg. Nucl. Chem.*, **37**, 1304 (1975).
- I. A. Cohen and W. S. Caughey, *Biochemistry*, **7**, 636 (1968).
- P. Henry, *Inorg. Chem.*, **5**, 688 (1966); D. P. Feld'man and B. D. Matseevskii, *Kinet. Katal.*, **15**, 1452 (1974); *Chem. Abstr.*, **82**, 103752u (1975).
- G. Rainoni and A. D. Zuberbühler, *Chimia*, **28**, 67 (1974).
- J. H. Bayston and M. E. Winfield, *J. Catal.*, **3**, 123 (1964).
- (a) R. D. Gillard and D. A. Phipps, *J. Chem. Soc. A*, 1074 (1971); (b) R. D. Gillard and A. Spencer, *Discuss. Faraday Soc.*, **46**, 213 (1968); (c) R. D. Gillard and A. Spencer, *J. Chem. Soc. A*, 2718 (1969).
- T. Yarinio, T. Matsushita, I. Masuda, and K. Shinra, *Chem. Commun.*, 1317 (1970).
- J. H. Swinehart, *Inorg. Chem.*, **4**, 1069 (1965).
- A. Yamamoto, L. K. Phillips, and M. Calvin, *Inorg. Chem.*, **7**, 847 (1968).
- J. O. Alben, W. H. Fuchsman, C. A. Beaudreau, and W. S. Caughey, *Biochemistry*, **7**, 624 (1968).
- G. S. Hammond and C. S. Wu, *Adv. Chem. Ser.*, **77**, 186 (1968).
- C. D. Schmulback, C. C. Hinkley, C. Kolich, T. A. Ballantine, and P. J. Nassiff, *Inorg. Chem.*, **13**, 2026 (1974).
- T. B. Joyner and W. K. Wilmarth, *J. Am. Chem. Soc.*, **83**, 516 (1961).
- (a) M. M. Takui Khan and A. E. Martell, *J. Am. Chem. Soc.*, **91**, 4668 (1969); (b) E.-I. Ochiai, *J. Inorg. Nucl. Chem.*, **35**, 3375 (1973); (c) J. S. Valentine,

- Chem. Rev.* **73**, 235 (1973); (d) F. Basolo, B. M. Hoffman, and J. A. Ibers, *Acc. Chem. Res.*, **8**, 384 (1975).
- (20) C. S. Arcus, J. L. Wilkinson, C. Mealli, T. J. Marks, and J. A. Ibers, *J. Am. Chem. Soc.*, **96**, 7564 (1974); S. J. Kim and T. Takizawa, *J. Chem. Soc., Chem. Commun.*, 356 (1974); R. Kellerman, P. J. Hulta, and K. Klier, *J. Am. Chem. Soc.*, **96**, 5946 (1974); S. K. Cheung, C. J. Grimes, J. Wong, and C. A. Reed, *ibid.*, **98**, 5028 (1976); C. J. Weschler, B. M. Hoffman, and F. Basolo, *ibid.*, **97**, 5278 (1975).
- (21) M. Calligaris, G. Nardin, L. Randaccio, and G. Tauzher, *Inorg. Nucl. Chem. Lett.*, **9**, 419 (1973); G. A. Rodley and W. T. Robinson, *Nature (London)*, **235**, 438 (1972).
- (22) A. L. Crumbliss and F. Basolo, *J. Am. Chem. Soc.*, **92**, 55 (1970).
- (23) G. Amiconi, M. Brunori, E. Anontini, G. Tauzher, and G. Costa, *Nature (London)*, **228**, 549 (1970).
- (24) G. Costa, G. Mestioni, G. Tauzher, and L. Stefani, *J. Organomet. Chem.*, **6**, 181 (1966).
- (25) F. Feigl, "Spot Tests in Inorganic Analysis", American Elsevier, New York, 1958, p 355.
- (26) (a) W. C. Schumb, C. N. Satterfield, and R. L. Wentworth, "Hydrogen Peroxide", Reinhold, New York, 1955, pp 404, 553; (b) *ibid.*, pp 386-388.
- (27) Made by a similar procedure as for the bromide salt according to Costa et al.²⁴ See Experimental Section.
- (28) The program used was a polynomial least-squares fit of data to $y = ax^n + bx^{n-1} + \dots$ where n could be assigned any integral value from 2 to 9. The program also included a plot that displayed the fit of the expression to the data. In all cases eighth- or ninth-order polynomials were used and the fit was excellent as shown by the plots and the low standard deviations (usually <2% of the points of lowest value). By-hand slopes of the carefully drawn reaction curves were measured using a straight-edge butted up against a glass rod that served to exaggerate the curvature around the locality of a desired point and aid in determining the tangent to the curve. The slopes thus obtained were found to agree very closely with the calculated values.
- (29) P. R. Bevington, "Data Reduction and Error Analysis for the Physical Sciences", McGraw-Hill, New York, 1969, Chapter 6.
- (30) The equations used are
- $$\text{rate} = k'[\text{HOAc}]_{\text{cor}}^{2.39} [\text{"product"}]^n$$
- $$\log \left(\frac{\text{rate}}{[\text{HOAc}]_{\text{cor}}^{2.39}} \right) = \log k' + n \log [\text{"product"}]$$
- (31) See paragraph at end of paper regarding supplementary material.
- (32) L. M. Mukherjee and R. S. Schultz, *Talanta*, **19**, 708 (1972).
- (33) M. Bos and E. A. M. F. Dahmen, *Anal. Chim. Acta*, **55**, 285 (1971).
- (34) (a) G. M. Barrow, *J. Am. Chem. Soc.*, **78**, 5802 (1956); (b) S. L. Johnson and K. A. Rumon, *J. Phys. Chem.*, **69**, 74 (1965).
- (35) D. S. Burgess and C. A. Kraus, *J. Am. Chem. Soc.*, **70**, 706 (1948); W. F. Luder and C. A. Kraus, *ibid.*, **69**, 2481 (1947).
- (36) M. M. Davis in "The Chemistry of Nonaqueous Solvents", J. J. Lagowski, Ed., Academic Press, New York, 1970, pp 78-85, and references cited therein.
- (37) The two OH stretch absorptions of acetic acid in pyridine are thought to arise from "tunnelling" in a double-minimum potential well possessing a low-energy barrier between the tautomeric forms py . . . HOAc and pyH . . . OAc. Also, $\text{H}(\text{OAc})_2^-$ ion has a very broad, almost indiscernible OH stretch at low wavenumber. See ref 34b and 38.
- (38) D. Hadzi, *Pure Appl. Chem.*, **11**, 435 (1965).
- (39) I. M. Kolthoff and M. K. Chantooni, Jr., *J. Phys. Chem.*, **66**, 1675 (1962).
- (40) I. M. Kolthoff and M. K. Chantooni, Jr., *J. Am. Chem. Soc.*, **87**, 4428 (1965).
- (41) I. M. Kolthoff and M. K. Chantooni, Jr., *J. Am. Chem. Soc.* **85**, 426 (1963); *J. Phys. Chem.*, **66**, 1675 (1962).
- (42) H. van der Heijde, *Anal. Chim. Acta*, **16**, 392 (1957).
- (43) HOAc (12 vol %) in pyridine has a dielectric constant of 13.1 compared with 12.9 for pyridine itself: Yu. Ya. Fialkov Borovikov, *Zh. Obshch. Khim.*, **36**, 1554 (1966); *Chem. Abstr.*, **66**, 50098w (1967).
- (44) Based on the energy in kcal/mol of the charge-transfer band in the visible spectrum of 1-ethyl-4-carbomethoxypyridinium iodide: E. M. Kosower, *J. Am. Chem. Soc.*, **80**, 3253, 3267 (1958); "An Introduction to Physical Organic Chemistry", Wiley, New York, 1968, pp 293-333.
- (45) The change in Z value over this range was measured in this work as 0.4 kcal/mol. If it is assumed that the reaction is actually second order in HOAc and that the remaining 0.39 order represents the "solvent" effect, then this corresponds to an increase in the rate constant of about 2.5-3-fold. To achieve the same rate increase in the $\text{S}_{\text{N}}2$ reaction of pyridine with ethyl iodide in alcoholic solvents requires an increase in Z of 15 kcal/mol. Likewise, the reaction of labeled iodide with methyl iodide requires a decrease in Z of about 3 kcal/mol (see ref 44).
- (46) The ratio K_4/K_2 was taken as 1.5 based on the data for the tetra-*n*-butylammonium salts in pyridine.³⁵
- (47) G. McLendon and A. E. Martell, *Coord. Chem. Rev.*, **19**, 1 (1976).
- (48) M. J. Carter, D. P. Riellemma, and F. Basolo, *J. Am. Chem. Soc.*, **96**, 392 (1974).
- (49) (a) M. Mori and J. A. Weil, *J. Am. Chem. Soc.*, **89**, 3732 (1967); (b) M. Mori, J. A. Weil, and M. Ishiguro, *ibid.*, **90**, 615 (1968); (c) J. H. Bayston and M. E. Winfield, *J. Catal.*, **3**, 123 (1964).
- (50) U. Thewalt and R. Marsh, *J. Am. Chem. Soc.*, **89**, 6364 (1967).
- (51) A. B. Hoffman and H. Taube, *Inorg. Chem.*, **7**, 1971 (1968); J. Simplicio and R. G. Wilkins, *J. Am. Chem. Soc.*, **91**, 1325 (1969).
- (52) A. Hair and W. K. Wilmarth, *J. Am. Chem. Soc.*, **83**, 509 (1961); J. H. Bayston, R. N. Beale, N. K. King, and M. E. Winfield, *Aust. J. Chem.*, **16**, 954 (1963).
- (53) Y. Abe and G. Wada, *Bull. Chem. Soc. Jpn.*, **47**, 2655 (1974).
- (54) D. Mersel, H. Levanon, and G. Czapski, *J. Phys. Chem.*, **78**, 779 (1974); G. Czapski, *Isr. J. Chem.*, **10**, 987 (1972), and references cited therein; D. Mersel, G. Czapski, and A. Samuni, *J. Am. Chem. Soc.*, **95**, 4148 (1973).
- (55) These signals are typical of BLCoO_2 where B is an axial ligand and L is an equatorial chelating ligand. See, for example, B. M. Hoffman, D. L. Diemente, and F. Basolo, *J. Am. Chem. Soc.*, **92**, 61 (1970).
- (56) C. E. Boozer, G. S. Hammond, C. E. Hamilton, and J. N. Sen, *J. Am. Chem. Soc.*, **77**, 3233 (1955).
- (57) E. W. Abel, J. M. Pratt, R. Whelan, and P. J. Wilkinson, *J. Am. Chem. Soc.*, **96**, 7119 (1974).
- (58) G. M. Coppinger, *J. Am. Chem. Soc.*, **79**, 2758 (1957).
- (59) F. A. Walker, D. Beroiz, and K. M. Kadish, *J. Am. Chem. Soc.*, **98**, 3484 (1976).
- (60) W. J. Wallace, J. C. Maxwell, and W. S. Caughey, *Biochem. Biophys. Res. Commun.*, **57**, 1104 (1974).
- (61) J. P. Collman, R. R. Gagne, C. A. Reed, T. R. Halbert, G. Lang, and W. T. Robinson, *J. Am. Chem. Soc.*, **97**, 1427 (1975).
- (62) G. W. Everett, Jr., and R. H. Holm, *J. Am. Chem. Soc.*, **88**, 2442 (1966); **87**, 2117 (1965).
- (63) A. E. Martell, R. L. Belford, and M. Calvin, *J. Inorg. Nucl. Chem.*, **5**, 170 (1958).
- (64) N. S. Gill and R. S. Nyholm, *J. Chem. Soc.*, 3997 (1959).
- (65) M. S. Kharasch and B. S. Joshi, *J. Org. Chem.*, **22**, 1439 (1957).
- (66) E. Wilhelm and R. Battino, *Chem. Rev.*, **73**, 1 (1973).